Fast and Accurate Seismic Computations in Laterally Varying Environments

MICHAEL D. COLLINS, (Member, IEEE), **JOSEPH F. LINGEVITCH**, AND **DAVID C. CALVO**
Naval Research Laboratory, Washington, DC 20375, USA

Corresponding author: Michael D. Collins (michael.collins@nrl.navy.mil)

ABSTRACT The parabolic equation method provides an unrivaled combination of computational efficiency and accuracy for wave propagation problems in the geosciences in which the environment has strong vertical variations and gradual horizontal variations. The development of this approach has been an active area of research for several decades in ocean acoustics, which includes problems involving sediment layers and ice cover that support shear waves. It is demonstrated here that this progress has culminated in a parabolic equation model for fast and accurate seismic computations in laterally varying environments. The model is tested for problems involving sloping boundaries and interfaces, variable layer thickness, continuous variations of the elastic parameters within layers, and a Rayleigh wave propagating along variable topography. The seismic parabolic equation model is based on an outgoing wave equation and rational approximations of operators for generating initial conditions, propagating the solution through stratified regions that approximate a laterally varying environment, and estimating transmitted fields across the vertical interfaces between regions.

I. INTRODUCTION

An accurate and efficient computational engine for modeling the propagation of compressional and shear waves in heterogeneous solids is essential for solving many problems in seismology, such as estimating the epicenter of an earthquake or the thicknesses and compositions of geologic layers. When the wave speeds, density, and locations of interfaces depend only on the depth below a reference level, solutions may be obtained with methods based on separation of variables. For many problems in seismology, however, it is necessary to also take into account lateral (horizontal) variations in the elastic parameters; this type of heterogeneity is often referred to as range dependence. Even when energy is assumed to propagate away from a source without coupling between planes of constant azimuth (a two-dimensional approximation that is appropriate for many problems), it may be challenging to obtain accurate solutions in environments that are range dependent and large in scale relative to a wavelength.

The associate editor coordinating the review of this manuscript and approving it for publication was Jing Yan.

Range-dependent problems may be solved with the finite-element method, which involves a linear system of equations to be solved over a computational grid that covers the entire domain and may consist of many thousands of grid points. When solving the system directly, run times increase nonlinearly with the number of grid points, and calculations quickly become impractical as the size of the domain increases. As illustrated in Fig. 1, for example, the total number of operations is on the order m^4 in the solution of a scalar frequency-domain wave equation on an $m \times m$ computational grid. Efficiency may be improved by using an iterative solver, but run times may still be prohibitive for large-scale problems. The amount of memory that is required for such computations may also be a limiting factor.

Range-dependent problems may also be solved with the parabolic equation method [1], which is based on factoring the operator in the wave equation, using one of the factors to obtain a parabolic wave equation that accounts for outgoing energy that propagates away from the source, and neglecting incoming energy that is back scattered toward the source. Run times increase only linearly with the number of grid points
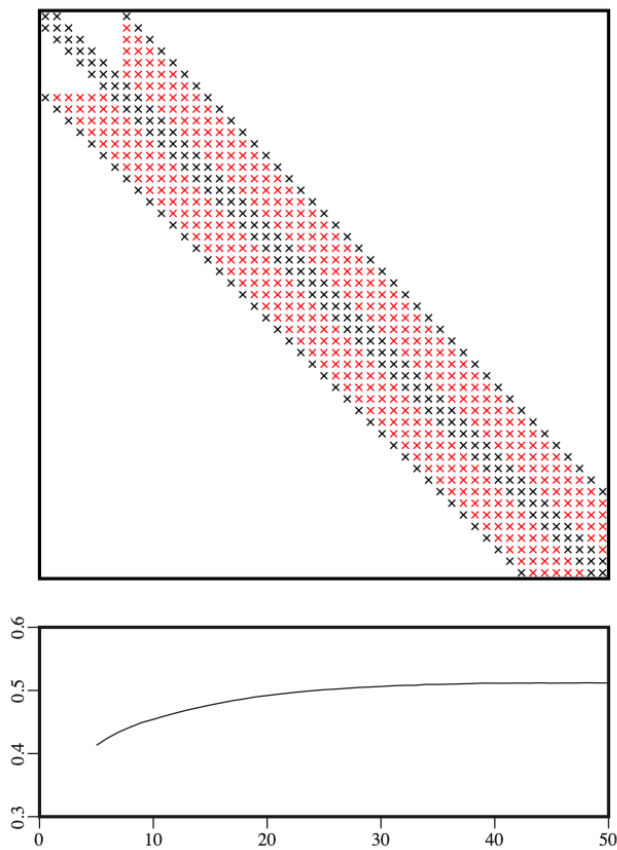
FIGURE 1. Numerical solution of the Helmholtz equation in which the columns of an $m \times m$ grid are stacked into a solution vector. Top: In the sparse matrix (shown here for $m = 7$) that corresponds to the standard difference approximation of the differential operator, non-zero entries (indicated by black crosses) are confined to five diagonals. During Gaussian elimination, other diagonals become populated with non-zero entries (indicated by red crosses). Bottom: The ratio of m^4 and the number of operations (additions, subtractions, multiplications, and divisions) required to solve the system for $5 \leq m \leq 50$. This curve was obtained by explicitly solving the system and counting operations that modify entries.

for this approach, which does not involve iterations, requires memory for only a small fraction of the grid, is often orders of magnitude faster than the finite-element method, and may be used to generate solutions on computational domains that span billions of square wavelengths [2]. Improved computational efficiency often comes at the expense of accuracy, but the parabolic equation method provides accurate solutions when range dependence is sufficiently gradual and outgoing energy dominates incoming energy. Although the parabolic equation method is based on one-way wave equations, solutions generated with this approach have been used in ocean acoustics applications that involve back-scattered energy from features on the seafloor [3] and schools of fish [4].

The parabolic equation method was initially applied to model the propagation of radio waves in the atmosphere [5]. The first applications to scalar wave propagation problems in seismology [6], [7] and ocean acoustics [8]–[10] came in

the 1970s. Shortly thereafter, there were attempts to extend the approach to the elastic wave equation [11]–[14], but the first successful implementations for this case were delayed until difficulties related to stability and factoring the operator (which do not arise for the scalar case) were understood and resolved [15]–[18]. During the decades that followed, there were further developments in the parabolic equation method for problems involving solid layers, including the construction of initial conditions for the parabolic wave equation [19], [20] and the accurate treatment of sloping interfaces and boundaries [21], [22]. Much of this work focused on problems in ocean acoustics that involve sediment layers that support shear waves or ice cover. It is demonstrated here that this progress has culminated in a model for fast and accurate seismic computations in laterally varying environments.

II. PARABOLIC EQUATION TECHNIQUES
A. THE PARABOLIC WAVE EQUATION

We derive here a parabolic wave equation for the case of an elastic medium in two dimensions. We work in the frequency domain in Cartesian geometry, where the range x is the horizontal distance from a source and z is the depth below a reference level. The treatment of the more realistic case of cylindrical geometry includes an additional factor to account for cylindrical spreading [1]. Substituting the equations for Hooke's Law into the momentum equations [23] in a medium in which the wave speeds and density are piece-wise continuous functions of depth, we obtain

$$(\lambda + 2\mu)\frac{\partial^2 u}{\partial x^2} + \frac{\partial}{\partial z}\left(\mu\frac{\partial u}{\partial z}\right) + \rho\omega^2 u$$
$$+ (\lambda + \mu)\frac{\partial^2 w}{\partial x \partial z} + \frac{\partial \mu}{\partial z}\frac{\partial w}{\partial x} = 0, \qquad (1)$$
$$\mu\frac{\partial^2 w}{\partial x^2} + \frac{\partial}{\partial z}\left((\lambda + 2\mu)\frac{\partial w}{\partial z}\right) + \rho\omega^2 w$$
$$+ (\lambda + \mu)\frac{\partial^2 u}{\partial x \partial z} + \frac{\partial \lambda}{\partial z}\frac{\partial u}{\partial x} = 0, \qquad (2)$$

where u and w are the horizontal and vertical displacements, λ and μ are the Lamé parameters, ρ is the density, and ω is the circular frequency. The compressional and shear wave speeds c_p and c_s are related to the coefficients of Eqs. (1) and (2) by $\rho c_p^2 = \lambda + 2\mu$ and $\rho c_s^2 = \mu$. Attenuation may be taken into account by allowing the wave speeds to be complex.

A parabolic wave equation is derived by factoring the operator in a wave equation into a product of an operator that corresponds to energy propagating outward in range (away from the source) and an operator that corresponds to incoming energy. Due to terms involving single range derivatives of the dependent variables, the vector operator defined in Eqs. (1) and (2) does not readily factor. Taking the range derivative of Eq. (1) and defining the new dependent variable

$U = \partial u / \partial x$, we obtain

$$(\lambda + 2\mu) \frac{\partial^2 U}{\partial x^2} + \frac{\partial}{\partial z} \left(\mu \frac{\partial U}{\partial z} \right) + \rho \omega^2 U$$

$$+ (\lambda + \mu) \frac{\partial^3 w}{\partial x^2 \partial z} + \frac{\partial \mu}{\partial z} \frac{\partial^2 w}{\partial x^2} = 0, \tag{3}$$

$$\mu \frac{\partial^2 w}{\partial x^2} + \frac{\partial}{\partial z} \left((\lambda + 2\mu) \frac{\partial w}{\partial z} \right) + \rho \omega^2 w$$

$$+ (\lambda + \mu) \frac{\partial U}{\partial z} + \frac{\partial \lambda}{\partial z} U = 0. \tag{4}$$

These equations are in the form,

$$\left(L \frac{\partial^2}{\partial x^2} + M \right) \mathbf{U} = 0, \tag{5}$$

where $\mathbf{U} = (U, w)$ and the entries of the 2×2 matrices L and M are depth operators. Inverting L and factoring the operator, we obtain

$$\left(\frac{\partial}{\partial x} - iT^{1/2} \right) \left(\frac{\partial}{\partial x} + iT^{1/2} \right) \mathbf{U} = 0, \tag{6}$$

where $T = L^{-1}M$. Assuming that outgoing energy dominates, we obtain the outgoing parabolic wave equation,

$$\frac{\partial \mathbf{U}}{\partial x} = iT^{1/2} \mathbf{U}. \tag{7}$$

B. RATIONAL APPROXIMATIONS

Numerical solutions may be obtained after approximating the operator square root. Expanding about a horizontal plane wave corresponding to the reference wave number k_0 and rearranging, we obtain

$$\frac{\partial \mathbf{U}}{\partial x} = ik_0 (1 + X)^{1/2} \mathbf{U}, \tag{8}$$

$$X = \frac{T - k_0^2}{k_0^2}. \tag{9}$$

Substituting an n-term rational approximation of the square root function into Eq. (8), we obtain

$$\frac{\partial \mathbf{U}}{\partial x} = ik_0 \left(1 + \sum_{j=1}^{n} \frac{a_{j,n} X}{1 + b_{j,n} X} \right) \mathbf{U}. \tag{10}$$

This equation may be solved numerically by applying Galerkin's method to discretize the depth operator [20] and the splitting method and Crank-Nicolson integration to march the solution in range.

For many scalar problems, accurate solutions may be obtained with the Padé approximations [24],

$$(1 + X)^{1/2} \cong 1 + \sum_{j=1}^{n} \frac{a_{j,n} X}{1 + b_{j,n} X} = \prod_{j=1}^{n} \frac{1 + c_{j,n} X}{1 + b_{j,n} X}, \tag{11}$$

$$a_{j,n} = \frac{2}{2n+1} \sin^2 \left(\frac{j\pi}{2n+1} \right), \tag{12}$$

$$b_{j,n} = \cos^2 \left(\frac{j\pi}{2n+1} \right), \tag{13}$$

$$c_{j,n} = \sin^2 \left(\frac{j\pi}{2n+1} \right), \tag{14}$$

which do not provide stable solutions for problems involving shear waves. The sum and product forms of the rational approximation are both useful in implementing the parabolic equation method.

For the seismic case, the most effective rational approximations that have been developed to date are the rotated rational approximations [25],

$$(1 + X)^{1/2} \cong 1 + \sum_{j=1}^{n} \frac{\tilde{a}_{j,n} X}{1 + \tilde{b}_{j,n} X} = \prod_{j=1}^{n} \frac{1 + \tilde{c}_{j,n} X}{1 + \tilde{b}_{j,n} X}, \tag{15}$$

$$\tilde{a}_{j,n} = \frac{e^{-i\theta/2} a_{j,n}}{\left(1 + b_{j,n} \left(e^{-i\theta} - 1 \right) \right)^2}, \tag{16}$$

$$\tilde{b}_{j,n} = \frac{e^{-i\theta} b_{j,n}}{1 + b_{j,n} \left(e^{-i\theta} - 1 \right)}, \tag{17}$$

$$\tilde{c}_{j,n} = \frac{e^{-i\theta} c_{j,n}}{1 + c_{j,n} \left(e^{-i\theta} - 1 \right)}, \tag{18}$$

which corresponds to a rotation around the branch point $X = -1$ by the angle θ. The Padé approximations correspond to matching $2n$ derivatives at $X = 0$. The rotated approximations correspond to matching $2n$ derivatives at $X = e^{i\theta} - 1$. For some problems, stable solutions may be obtained by using a small value of θ, but rotations of 90 degrees or more are required for some problems involving thin layers [26]. As the matching point moves farther from $X = 0$, which corresponds to horizontal wave numbers near k_0, it may be necessary to increase n in order to achieve the desired level of accuracy.

There are other strategies for designing rational approximations. For the rotated approximations, all of the constraints (matching derivatives) are moved (a substantial distance in some cases) away from $X = 0$. An alternative approach is to keep most of the constraints at $X = 0$ (the accuracy constraints) and use a few of the remaining constraints (the stability constraints) to prevent instabilities [18]. Another approach is to formally integrate Eq. (8) to obtain

$$\mathbf{U}(x + \Delta x, z) = \exp \left(ik_0 \Delta x (1 + X)^{1/2} \right) \mathbf{U}(x, z), \tag{19}$$

where Δx is the range step in the numerical solution. This equation may be solved by applying a rational approximation of the exponential of the square root [27]. This solution is identical in form to the Crank-Nicolson solution, but it has different coefficients (which must be determined numerically), is correct to higher order in the range numerics, and allows larger range steps (multiple wavelengths versus a fraction of a wavelength).

C. INITIAL CONDITIONS

The parabolic wave equation is an initial-value problem in range that requires an initial condition. The self-starter is an approach for generating an initial condition that is based on

rational approximations of operators [19]. For the case of a compressional point source at $z = z_0$ in cylindrical geometry, the self-starter is [20]

$$\mathbf{U}(r_0, z) = F_p \begin{pmatrix} k_p^2 \delta(z - z_0) + \delta''(z - z_0) \\ -\delta'(z - z_0) \end{pmatrix}, \qquad (20)$$

$$F_p = r_0^{-1/2}(1 + X)^{-1/4} \exp\left(ik_0 r_0 (1 + X)^{1/2}\right), \quad (21)$$

where r_0 is the initial range and $k_p = \omega/c_p$ is the compressional wave number at the source depth. For the case of a shear point source, the self-starter is [20]

$$\mathbf{U}(r_0, z) = F_s \begin{pmatrix} -\delta'(z - z_0) \\ \delta(z - z_0) \end{pmatrix}, \qquad (22)$$

$$F_s = r_0^{-1/2}(1 + X)^{1/4} \exp\left(ik_0 r_0 (1 + X)^{1/2}\right). \quad (23)$$

An approach described in Ref. 20 may be used to handle the delta function and its derivatives.

In order to avoid numerical problems associated with the singularity at the source depth, the self-starter may be implemented in a series of steps that involve an intermediate solution:

$$\mathbf{U}_0(z) = (1 + \gamma X)^{-2}$$
$$\times \begin{pmatrix} k_p^2 \delta(z - z_0) + \delta''(z - z_0) \\ -\delta'(z - z_0) \end{pmatrix}, \quad (24)$$

$$\mathbf{U}(r_0, z) = r_0^{-1/2}(1 + X)^{-1/4}(1 + \gamma X)^2$$
$$\times \exp\left(ik_0 r_0 (1 + X)^{1/2}\right) \mathbf{U}_0(z), \qquad (25)$$

where γ is chosen so that the inverse of the operator is non-singular (the value $\gamma = i$ has been proven to be effective without fail for a wide range of problems). In previous implementations of the self-starter, a single rational approximation was used for all three of the factors in the operator on the right side of Eq. (25). With this approach, the coefficients must be determined numerically, and the algorithm for finding them may fail to converge in some cases. We apply here an alternative approach that does not require searching for coefficients. The factor on the right is the propagator that appears in Eq. (19). This factor may be taken into account by using the rotated rational approximations and Crank-Nicolson integration to advance the intermediate solution out to $r = r_0$. The next factor may be taken into account by two applications of the operator. The remaining factor is the fourth root, which may be approximated in terms of a rational approximation. Since this factor does not depend on the range step, it may be handled efficiently by obtaining rational approximations for the fourth root and saving them (it is not necessary to generate them each time the parabolic wave equation is solved).

D. ACCURATE TREATMENT OF RANGE DEPENDENCE

A range-dependent problem may be handled by dividing the environment into a series of range-independent regions and using the parabolic wave equation to propagate the field through each region. All that remains is to estimate the transmitted fields at the vertical interfaces between regions, where the exact solution satisfies continuity of u, w, the normal stress σ_{xx}, and the tangential stress σ_{xz}. Since there is only one range derivative in the parabolic wave equation, its solutions cannot satisfy all four conditions, but accurate solutions may be obtained for many problems by solving a scattering problem at each vertical interface, discarding the back-scattered field, and using the transmitted field as an initial condition in the next region. The stresses are related to the dependent variable in terms of the equations [21],

$$\begin{pmatrix} \sigma_{xx} \\ w \end{pmatrix} = R\mathbf{U}, \qquad (26)$$

$$\begin{pmatrix} u \\ -\sigma_{xz} \end{pmatrix} = -iST^{-1/2}\mathbf{U}, \qquad (27)$$

$$R = \begin{pmatrix} \lambda + 2\mu & \lambda \dfrac{\partial}{\partial z} \\ 0 & 1 \end{pmatrix}, \qquad (28)$$

$$S = \begin{pmatrix} 1 & 0 \\ \lambda \dfrac{\partial}{\partial z} + \dfrac{\partial \lambda}{\partial z} & \dfrac{\partial}{\partial z}(\lambda + 2\mu)\dfrac{\partial}{\partial z} + \rho\omega^2 \end{pmatrix}. \qquad (29)$$

Conservation of the displacements and stresses across a vertical interface between range-independent regions A and B corresponds to the conditions,

$$R_B\mathbf{U}_t = R_A(\mathbf{U}_i + \mathbf{U}_r), \qquad (30)$$

$$S_B T_B^{-1/2}\mathbf{U}_t = S_A T_A^{-1/2}(\mathbf{U}_i - \mathbf{U}_r), \qquad (31)$$

where the subscripts i, r, and t denote the incident, reflected, and transmitted fields, the subscripts A and B denote evaluation in the respective regions, and the negative sign reflects the fact that $\mathbf{U}_r$ is incoming. From Eqs. (30) and (31), we obtain

$$\mathbf{U}_t = \frac{1}{2}\left(R_B^{-1}R_A + T_B^{1/2}S_B^{-1}S_A T_A^{-1/2}\right)\mathbf{U}_i$$
$$+ \frac{1}{2}\left(R_B^{-1}R_A - T_B^{1/2}S_B^{-1}S_A T_A^{-1/2}\right)\mathbf{U}_r. \quad (32)$$

Applying the assumptions that range dependence is gradual and the outgoing field dominates, we drop the second term on the right side of Eq. (32), which is small to second order under the assumptions, and obtain the single-scattering approximation [21],

$$\mathbf{U}_t = \frac{1}{2}\left(R_B^{-1}R_A + T_B^{1/2}S_B^{-1}S_A T_A^{-1/2}\right)\mathbf{U}_i. \qquad (33)$$

This approach for handling the interfaces between range-independent regions has been found to provide accurate solutions for a wide range of problems involving sloping solid-solid interfaces. It may be applied to the case of a sloping boundary by placing an artificial material with low density above the boundary and treating the boundary as an interface.
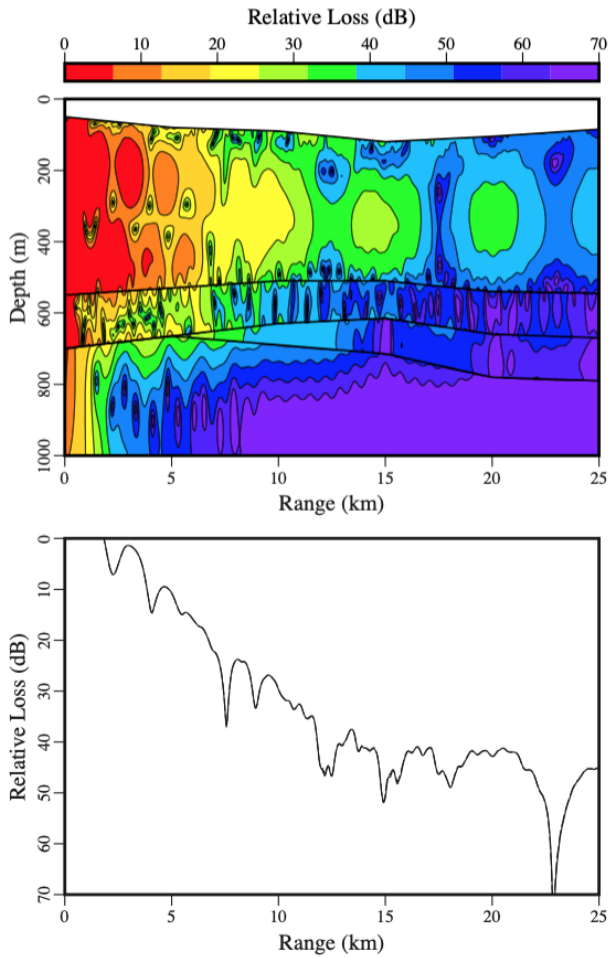
FIGURE 2. Top: Compressional transmission loss for a problem involving variable topography, sloping interfaces, and variable layer thickness. Bottom: Compressional transmission loss at $z = 180$ m generated with the parabolic equation method (solid curve) is nearly identical to the solution generated with a finite-element model (dashed curve), and thus it is difficult to see both curves.

FIGURE 3. Top: Compressional transmission loss for a problem involving variable topography, a sloping interface, and a Rayleigh wave. Bottom: Compressional transmission loss at $z = 220$ m generated with the parabolic equation method (solid curve) is nearly identical to the solution generated with a finite-element model (dashed curve).

E. COMPRESSIONAL AND SHEAR POTENTIALS

In a homogeneous layer, the compressional and shear potentials ϕ and ψ are defined by [20]

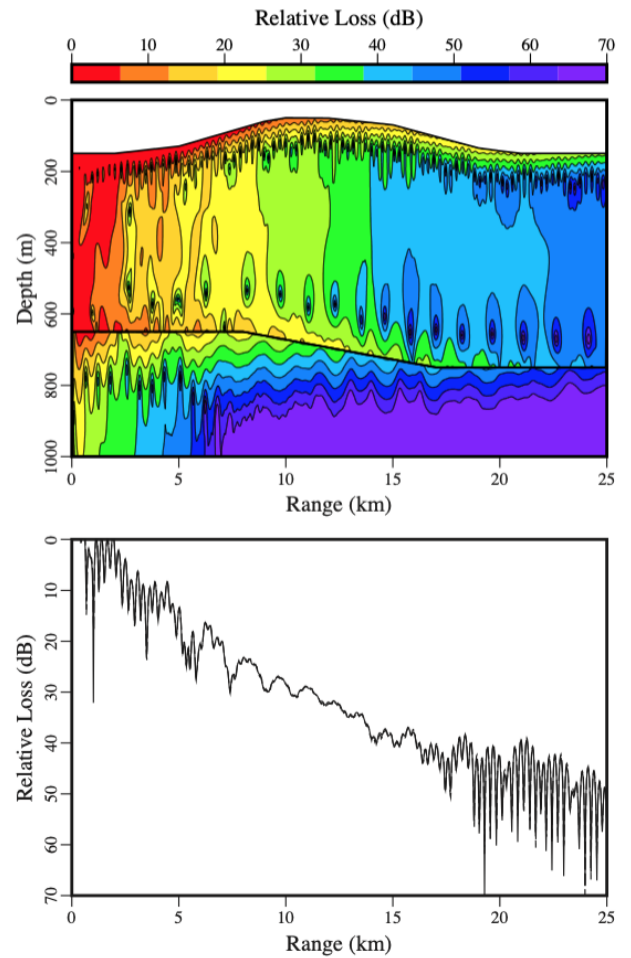$$\rho \omega^2 \begin{pmatrix} \phi \\ \psi_x \end{pmatrix} = -Q\mathbf{U}, \tag{34}$$

$$Q = \begin{pmatrix} \lambda + 2\mu & (\lambda + 2\mu)\dfrac{\partial}{\partial z} \\ (\lambda + 2\mu)\dfrac{\partial}{\partial z} & (\lambda + 2\mu)\dfrac{\partial^2}{\partial z^2} + \rho\omega^2 \end{pmatrix}, \tag{35}$$

where $\psi_x = \partial \psi / \partial x$. We define the compressional and shear transmission losses,

$$TL_p = -20\log_{10}|\phi|, \tag{36}$$

$$TL_s = -20\log_{10}|\psi_x|. \tag{37}$$

One could alternatively define the shear transmission loss in terms of ψ, which may be obtained by applying the inverse of

the square root operator before applying Q on the right side of Eq. (34).
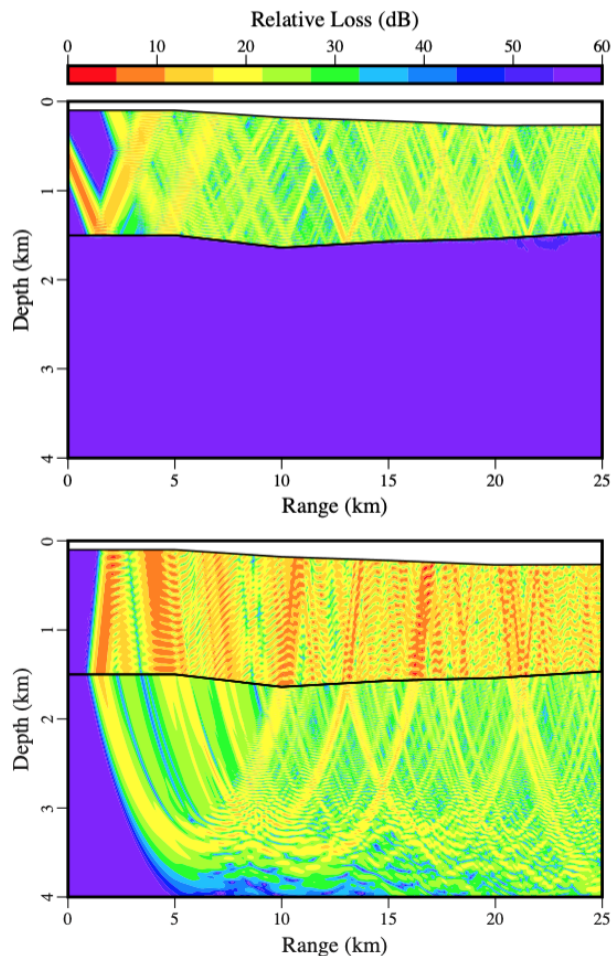
III. TEST CASES

Parabolic equation techniques for generating initial conditions, marching the solution in range, and accurately handling sloping interfaces and other types of range dependence were originally developed for ocean acoustics problems but are adapted and tested here for seismic problems. The accuracy of these techniques is demonstrated for examples involving variable topography, sloping interfaces, and other effects by making comparisons with solutions generated with a finite-element model [28]. Some of the details of the examples are specified in the supplemental material, including the depth dependence of the wave speeds, density, and attenuation and the range dependence of the topography and layer thicknesses. For each of the examples, we include an attenuating layer deep in the grid to prevent non-physical reflections from the bottom boundary.
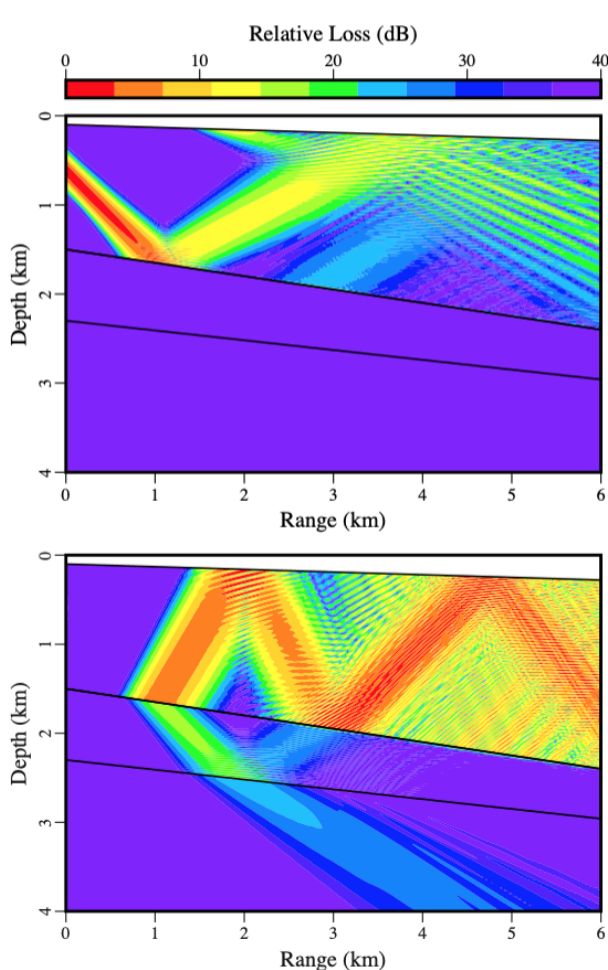
FIGURE 4. Compressional transmission loss (top) and shear transmission loss (bottom) for a problem involving variable topography, sloping interfaces, and variable layer thickness. An array of sources is beamed 45 degrees below the horizontal, and there is coupling between compressional and shear waves at the boundary and interfaces.

FIGURE 5. Compressional transmission loss (top) and shear transmission loss (bottom) for a problem involving variable topography, a sloping interface, variable layer thickness, and wave speed gradients in the lower layer. An array of sources is beamed 30 degrees below the horizontal, and shear waves are refracted in the lower layer.

The first two examples involve a 5 Hz compressional point source (cylindrical geometry) and a maximum range of 25 km. For example A, topography varies by 70 m, and there are three layers overlying a half space. The thickness of the top layer ranges from 390 to 500 m. The thickness of the second layer ranges from 105 to 150 m. The thickness of the third layer ranges from 0 to 120 m. The source is at $z = 500$ m (450 m below the boundary). In Fig. 2, the color plot indicates substantial interactions with the boundary and interfaces, and the parabolic equation and finite-element solutions are nearly identical at $z = 180$ m. For example B, topography varies by 100 m, and there is one layer overlying a half space. The depth of the interface is $z = 650$ m for $r < 8$ km, $z = 750$ m for $r > 17$ km, and linearly sloping between these values for 8 km $< r < 17$ km. The source at $z = 155$ m (5 m below the boundary) excites a Rayleigh wave, which propagates along the sloping topography. In Fig. 3, the color plot shows a rapid interference pattern between the Rayleigh wave near the boundary and modes within the layer, and

the parabolic equation and finite-element solutions are nearly identical at $z = 220$ m.

It is often possible to estimate the local layer structure from energy that propagates vertically (or at steep angles) and returns to the surface after reflecting from interfaces. There have been applications of the parabolic equation method to this problem in which depth is taken to be the marching direction (the operator is factored into down going and up going operators). With this approach, variations in the elastic parameters are not gradual in the vertical direction at an interface. This complication may be avoided by using the range-marching parabolic equation. This approach is not applicable when energy propagates directly downward, but it is applicable if there is range separation between the source and receiver. The purpose of example C is to illustrate the application of the parabolic equation method to this type of problem.

The environment for example C consists of two layers overlying a half space. The boundary and interfaces have

constant downslopes for $0 < x < 6$ km, with endpoints of $z = 100$ m and $z = 280$ m for the boundary, $z = 1500$ m and $z = 2400$ m for the first interface, and $z = 2300$ m and $z = 2960$ m for the second interface. An array of forty compressional line sources (Cartesian geometry) in the upper layer is beamed at 45 degrees below the horizontal at 50 Hz. The jth source is located at $z = [307.5 + (j - 1) 15]$ m and has a Gaussian weighted phase factor. In Fig. 4, the compressional wave beam at the first interface gives rise to a transmitted shear wave beam and both types of reflected beam. Several other beams are generated from interactions with the boundary and interfaces. By using an appropriate choice for k_0, it would be possible to handle waves that propagate at much steeper angles. In practice, this type of scenario could be handled by constructing time series by Fourier synthesis of solutions of the parabolic wave equation.

The purpose of example D is to illustrate the efficiency of the parabolic equation method when the combination of the frequency and the dimensions of the environment is such that running a finite-element model may not be practical. The field is generated by the same array of 50 Hz sources as an example C, with the exception that the beam is steered to 30 degrees below the horizontal. The environment has variable topography, a layer overlying a half space, a sloping interface, and wave speed gradients in the half space. In Fig. 5, the shear wave beams in the half space are refracted by the shear speed gradient. If the dimensions of the computational domain and the number of grid points per wavelength remain constant but the frequency is increased by a factor of ten, the run time should increase by a factor of 10^4 for a finite-element model that is based on a direct solver but only by a factor of 10^2 for a parabolic equation model. We did not attempt to run a finite-element model for example D, but running a parabolic equation model for this problem took less than a minute on an Apple MacBook Pro with a 2.8 GHz Intel Core i7 processor.

IV. DISCUSSION

For many wave propagation problems of interest in the geosciences, it is necessary to account for horizontal variations in the environment. The parabolic equation method provides an excellent combination of accuracy and efficiency for such range-dependent problems. Approaches for generating initial conditions, propagating the field through range-independent regions, and estimating transmitted fields across the interfaces between regions have been implemented in a seismic parabolic equation model. By making comparisons with solutions generated with a finite-element model, the accuracy of the model has been demonstrated for problems with sloping boundaries and interfaces, variable layer thickness, and the propagation of a Rayleigh wave along variable topography. The elastic parabolic equation is based on an unconventional formulation involving the vertical displacement and the horizontal derivative of the horizontal displacement, but the displacements, stresses, and potentials may be obtained with local conversion formulas. Various rational approximations have been proposed for obtaining accurate, efficient, and

stable solutions. In some cases, the coefficients must be determined with searches that may not converge, but the results presented here are based on coefficients that are known in analytic form or may be tabulated (and thus do not require a search for each run).

REFERENCES

[1] M. D. Collins and W. L. Siegmann, *Parabolic Wave Equations With Application*. Berlin, Germany: Springer, 2019.

[2] B. E. McDonald, M. D. Collins, W. A. Kuperman, and K. D. Heaney, "Comparison of data and model predictions for Heard Island acoustic transmissions," *J. Acoust. Soc. Amer.*, vol. 96, no. 4, pp. 2357–2370, Oct. 1994.

[3] N. C. Makris, L. Z. Avelino, and R. Menis, "Deterministic reverberation from ocean ridges," *J. Acoust. Soc. Amer.*, vol. 97, no. 6, pp. 3547–3574, Jun. 1995.

[4] N. C. Makris, P. Ratial, D. T. Symonds, S. Jagannathan, S. Lee, and R. W. Nero, "Fish population and behavior revealed by instantaneous continental shelf-scale imaging," *Science*, vol. 311, no. 5761, pp. 660–663, 2006.

[5] M. A. Leontovich and V. A. Fock, "Solution of the problem of propagation of electromagnetic waves along the earth's surface by the method of parabolic equation," *J. Express Theor. Phys.*, vol. 16, pp. 557–573, 1946.

[6] J. F. Claerbout, "Coarse grid calculations of waves in inhomogeneous media with application to delineation of complicated seismic structure," *Geophysics*, vol. 35, no. 3, pp. 407–418, 1970.

[7] T. Landers and J. F. Claerbout, "Numerical calculations of elastic waves in laterally inhomogeneous media," *J. Geophys. Res.*, vol. 77, pp. 1476–1483, Mar. 1972.

[8] R. H. Hardin and F. D. Tappert, "Applications of the split-step Fourier method to the numerical solution of nonlinear and variable coefficient wave equations," *SIAM Rev.*, vol. 15, no. 2, p. 423, 1973.

[9] S. M. Flatté and F. D. Tappert, "Calculation of the effect of internal waves on oceanic sound transmission," *J. Acoust. Soc. Amer.*, vol. 58, no. 6, pp. 1151–1159, Dec. 1975.

[10] F. D. Tappert, "The parabolic approximation method," in *Wave Propagation and Underwater Acoustics* (Lecture Notes in Physics), vol. 70, J. B. Keller and J. S. Papadakis, Eds. New York, NY, USA: Springer, 1977, pp. 224–287.

[11] J. J. McCoy, "A parabolic theory of stress wave propagation through inhomogeneous linearly elastic solids," *J. Appl. Mech.*, vol. 44, no. 3, pp. 462–468, Sep. 1977.

[12] J. A. Hudson, "A parabolic approximation for elastic waves," *Wave Motion*, vol. 2, no. 3, pp. 207–214, Sep. 1980.

[13] J. Corones, B. DeFacio, and R. J. Krueger, "Parabolic approximations to the time-independent elastic wave equation," *J. Math. Phys.*, vol. 23, no. 4, pp. 577–586, Apr. 1982.

[14] S. C. Wales and J. J. McCoy, "A comparison of parabolic wave theories for linearly elastic solids," *Wave Motion*, vol. 5, no. 2, pp. 99–113, Apr. 1983.

[15] R. R. Greene, "A high-angle one-way wave equation for seismic wave propagation along rough and sloping interfaces," *J. Acoust. Soc. Amer.*, vol. 77, no. 6, pp. 1991–1998, Jun. 1985.

[16] M. D. Collins, "A higher-order parabolic equation for wave propagation in an ocean overlying an elastic bottom," *J. Acoust. Soc. Amer.*, vol. 86, pp. 1459–1464, Oct. 1989.

[17] B. T. R. Wetton and G. H. Brooke, "One-way wave equations for seismo-acoustic propagation in elastic waveguides," *J. Acoust. Soc. Amer.*, vol. 87, pp. 624–632, Feb. 1990.

[18] M. D. Collins, "Higher-order Padé approximations for accurate and stable elastic parabolic equations with application to interface wave propagation," *J. Acoust. Soc. Amer.*, vol. 89, no. 3, pp. 1050–1057, Mar. 1991.

[19] M. D. Collins, "A self-starter for the parabolic equation method," *J. Acoust. Soc. Amer.*, vol. 92, no. 4, pp. 2069–2074, Oct. 1992.

[20] W. Jerzak, W. L. Siegmann, and M. D. Collins, "Modeling Rayleigh and Stoneley waves and other interface and boundary effects with the parabolic equation," *J. Acoust. Soc. Amer.*, vol. 117, no. 6, pp. 3497–3503, Jun. 2005.

[21] M. D. Collins, "A single-scattering correction for the seismo-acoustic parabolic equation," *J. Acoust. Soc. Amer.*, vol. 131, no. 4, pp. 2638–2642, Apr. 2012.

[22] M. D. Collins and A. Ramamurti, "Parabolic equation modeling of Scholte waves and other effects along sloping fluid-solid interfaces," *J. Theor. Comput. Acoust.*, vol. 29, no. 01, Mar. 2021, Art. no. 2050025.

[23] H. Kolsky, *Stress Waves Solids*. New York, NY, USA: Dover, 1963.

[24] A. Bamberger, B. Engquist, L. Halpern, and P. Joly, "Higher order paraxial wave equation approximations in heterogeneous media," *SIAM J. Appl. Math.*, vol. 48, no. 1, pp. 129–154, Feb. 1988.

[25] F. A. Milinazzo, C. A. Zala, and G. H. Brooke, "Rational square-root approximations for parabolic equation algorithms," *J. Acoust. Soc. Amer.*, vol. 101, no. 2, pp. 760–766, Feb. 1997.

[26] M. D. Collins, "Treatment of ice cover and other thin elastic layers with the parabolic equation method," *J. Acoust. Soc. Amer.*, vol. 137, no. 3, pp. 1557–1563, Mar. 2015.

[27] M. D. Collins, "A split-step Padé solution for the parabolic equation method," *J. Acoust. Soc. Amer.*, vol. 93, no. 4, pp. 1736–1742, Apr. 1993.

[28] *Multiphysics V. 5.2*, COMSOL AB, Stockholm, Sweden, 2017.

JOSEPH F. LINGEVITCH was born in Elmhurst, IL, USA, in 1964. He received the B.S. degree in physics from Bradley University, Peoria, IL, in 1986, the M.S. degree in physics from the University of Illinois at Urbana–Champaign, in 1989, and the Ph.D. degree in applied mathematics from Northwestern University, Evanston, IL, USA, in 1995. He has been with the Naval Research Laboratory, Washington, DC, since 1995. His research interests include acoustic propagation, signal processing, and inverse problems. He is a member of the Acoustical Society of America and the Skyline Soaring Club.

MICHAEL D. COLLINS (Member, IEEE) was born in Greenville, PA, USA, in 1958. He received the B.S. degree in mathematics from the Massachusetts Institute of Technology, Cambridge, MA, in 1982, and the Ph.D. degree in applied mathematics from Northwestern University, Evanston, IL, in 1988. He has been with the Naval Research Laboratory, since 1985, with assignments at the offices in Washington, DC, and the Stennis Space Center, Bay St. Louis, MS. His research interests include wave propagation, inverse problems, signal processing, ocean acoustics, and the Ivory-billed Woodpecker. He is a member of the Society for Industrial and Applied Mathematics and the American Geophysical Union.

DAVID C. CALVO received the Ph.D. degree in mechanical engineering from the Massachusetts Institute of Technology, in 2001. He is the Head of the Acoustic Signal Processing and Systems Branch, Acoustics Division, U.S. Naval Research Laboratory, Washington, DC, USA. His research interests include underwater acoustic propagation and scattering, acoustic sensing, sound isolation and transduction, acoustic metamaterials, numerical methods, marine electromagnetics, and nonlinear dispersive wave theory.

• • •